

Integrated spectral kurtosis analysis

Arvid Trapp* and Peter Wolfsteiner*

*Munich University of Applied Sciences, Munich, Germany

E-mail: arvid.trapp@hm.edu

Abstract—Spectral kurtosis (SK) analysis is a popular signal processing technique to locate harmonics, transients and repetitive impulses in the frequency domain. As a fourth-order frequency-domain technique the SK belongs to the wide range of higher-order spectral analysis and commonly finds application for the pre-processing of band-limited envelope analyses. We propose a novel definition of the SK, whereby SK estimates are fully resolved in time using the technique of filtering-averaging. Hereby, SK estimates are defined as the average of the full time resolution of trispectral estimates, while the latter can be processed to carry out envelope analyses directly on these estimates. Conjoining SK and envelope analysis specifies an integrated SK analysis, providing insight into the generating mechanisms of its estimates. It further differentiates from the popular short-time Fourier transform (STFT) estimator in a facilitated handling, (a) requiring less parameters, (b) circumventing the quasi-stationary assumption of the STFT, and (c) providing the frequency bandwidth with a clear meaning.

I. INTRODUCTION

A fundamental task of signal processing is to acquire meaningful information from physical recordings subjected to noise. Spectral kurtosis (SK) analysis is applied to identify the location of transients and impulsive components in the spectral domain. This commonly functions as a pre-processing technique for subsequent comprehensive analysis in the corresponding frequency bands. As such, the SK is popularly employed for selecting frequency bands in order to diagnose rolling element bearing damages by band-limited envelope analyses [1], [2].

The fundamental mechanism of the SK is to relate fourth- to second-order averages resolved for frequency bands. Hereby, stationary Gaussian noise is fully defined by the second-order (power) spectral density (PSD). Contrasting second- with fourth-order band-limited spectral estimates enables locating frequency bands that contain components distinct from stationary Gaussian noise, i.e. transients, significant harmonic components or repetitive impulsive characteristics (cyclo-stationarity). The SK originates from a heuristically introduced proposal based on the short-time Fourier transform (STFT) that was named frequency-domain kurtosis [3]. Antoni significantly contributed to today’s popularity by a profound formalization [4]. He adapted the STFT estimation scheme and the name spectral kurtosis [5], which has lend its denotation to the algorithms that are nowadays implemented in commercial tools.

From higher-order spectral (HOS) analysis [6] it is well known, that the kurtosis is a function of three arguments in the frequency domain. It represents the normalized spectral decomposition of the fourth-order central moment — the

trispectrum. Hereby, the SK defines a subset of the normalized cumulant trispectrum that encompasses all estimates for which the three frequency arguments refer exclusively to a single frequency band. Consequently, the SK drastically reduces the complexity of HOS analysis, which can certainly be identified as a central facet for the SK’s popularity.

For tracing varying components in the spectral domain, inherently linked to stationarity, the SK has commonly been estimated by short-time Fourier or wavelet analysis. By choosing an appropriate segmentation, these segment-wise stationary techniques allow to observe a fluctuating spectral decomposition along their evolution in time. This is processed by SK analysis to calculate frequency-selective averages of different orders. A recently published estimator for HOS [7] bypasses the segmentation in time adopting frequency-domain smoothing to obtain stable HOS estimates. Since these estimates are fully resolved in time this estimator enables direct envelope analysis on its estimates, enabling an integrated SK analysis.

II. STATISTICAL SIGNAL PROCESSING

According to the central limit theorem (CLT), random processes $X(t)$ that are influenced by a large set of individual, i.e. statistically independent, variables follow the Gaussian probability density,

$$p_g(x) = \frac{1}{\sqrt{2\pi}\sigma} e^{-\frac{1}{2}\left(\frac{x-\mu}{\sigma}\right)^2} \quad (1)$$

fully defined by mean μ and variance σ^2 . As a consequence of the CLT such processes have a random phase information $\varphi(f)$ with a statistically independent frequency-domain characteristic. Spectral analysis ($E[\cdot]$ — expected value)

$$S_n(f_1, \dots, f_{n-1}) = \lim_{T \rightarrow \infty} \frac{1}{T} E[X_T(f_1) \dots X_T(f_{n-1}) X_T(-f_1 - \dots - f_{n-1})] \quad (2)$$

processes the amplitude and the phase information of the (finite) Fourier transform $X_T(f)$. Its only exception is the second-order ($n = 2$) PSD $S_2(f)$, which is restricted to the amplitudes and hence phase-blind. A process tests positive for stationary Gaussian noise, if statistically independent phases, i.e. conformance with the CLT, are identified by applying higher-order ($n > 2$) spectra [8], [9]. As this hypothesis comprises considerable effort in practice, stationary Gaussian

noise is often assessed by a simplification using the scalar-valued central moments

$$\mu_n = E[(X(t) - E[X(t)])^n] = \int_{-\infty}^{\infty} (x - \mu)^n p(x) dx \quad (3)$$

Therefore, the kurtosis

$$\beta = \frac{\mu_4}{\sigma^4} = \frac{\mu_4}{(\mu_2)^2} \quad (4)$$

functions as a central indicator relating the fourth- to the second-order central moment. Since the fourth-order moment of a stationary Gaussian process is specified by $\mu_{4,g} = 3\mu_2^2$, the kurtosis can indicate deviations from a stationary Gaussian process whose value is $\beta_g = 3$. A popular alternative are cumulants c_n ($c_2 = \mu_2$; $c_4 = \mu_4 - 3\mu_2^2$; [10]), complementing the kurtosis with the excess kurtosis

$$\gamma = \frac{c_4}{(c_2)^2} = \frac{\mu_4 - 3\mu_2^2}{(\mu_2)^2} = \beta - 3 \quad (5)$$

Higher-order cumulants enjoy the property of being zero for stationary Gaussian processes, hence $\gamma_g = 0$. HOS $S_n(f_1, \dots, f_{n-1})$ and $C_n(f_1, \dots, f_{n-1})$ are the spectral decomposition of central moments resp. of cumulants

$$\begin{aligned} \mu_n &= \int_{-\infty}^{\infty} \dots \int_{-\infty}^{\infty} S_n(f_1, \dots, f_{n-1}) df_1 \dots df_{n-1} \\ c_n &= \int_{-\infty}^{\infty} \dots \int_{-\infty}^{\infty} C_n(f_1, \dots, f_{n-1}) df_1 \dots df_{n-1} \end{aligned} \quad (6)$$

From Eqs. (4) and (6) follows that the kurtosis is a function of three arguments in the frequency domain [11]

$$B(f_1, f_2, f_3) = \frac{S_4(f_1, f_2, f_3)}{\sqrt{S_2(f_1)S_2(f_2)S_2(f_3)S_2(-f_1 - f_2 - f_3)}} \quad (7)$$

The kurtosis function $B(f_1, f_2, f_3)$ is the normalized representation of the trispectrum $S_4(f_1, f_2, f_3)$ which — as a fourth-order spectrum — measures cross-frequency correlation of up to four frequencies f_1, \dots, f_4 , whereby $f_4 = -(f_1 + f_2 + f_3)$. The SK follows this frequency-decomposition principle. Hereby, it considers a subset of the full fourth-order set, which is spanned up between the Nyquist frequency f_{Ny} in Fig. 1 ($-f_{Ny} \leq f \leq f_{Ny}$). The SK is defined as the subset of the normalized cumulant trispectrum (replacing $S_4(f_1, f_2, f_3)$ with $C_4(f_1, f_2, f_3)$ in Eq. 7) that encompasses all estimates relating to a unique frequency (red in Fig. 1):

$$\{f_1 = f_2 = -f_3, f_1 = -f_2 = f_3, f_1 = -f_2 = -f_3\} \quad (8)$$

Each of these subsets is the intersection of two combinations of the set [12], [13],

$$\{f_1 + f_2 = 0, f_2 + f_3 = 0, f_3 + f_1 = 0\} \quad (9)$$

locating the so-named normal manifolds in the trispectral set (Fig. 1). In the following, those subsets relating exclusively to a unique frequency are denoted single-frequency moments

$$\mu_4(f) \hat{=} (\Delta f)^3 \Re[S_4(f, f, -f)]; \quad \mu_2(f) \hat{=} \Delta f S_2(f) \quad (10)$$

by inserting one of set (8) into the trispectrum, e.g. $S_4(f, f, -f)$. Defining the fourth-order single-frequency moment $\mu_4(f)$ by the real part comes from the complex-conjugated (Hermitian) symmetry at the origin characteristic for all spectra, e.g.

$$\begin{aligned} S_4(f_1, f_2, f_3) + S_4(-f_1, -f_2, -f_3) &= \\ 2\Re[S_4(f_1, f_2, f_3)] &= 2\Re[S_4(-f_1, -f_2, -f_3)] \end{aligned} \quad (11)$$

Consequently, specifying $\mu_4(f)$ as a one-sided, i.e. positive, frequency decomposition, the trispectral set contains six symmetric subsets with the redundant information of $\mu_4(f)$.

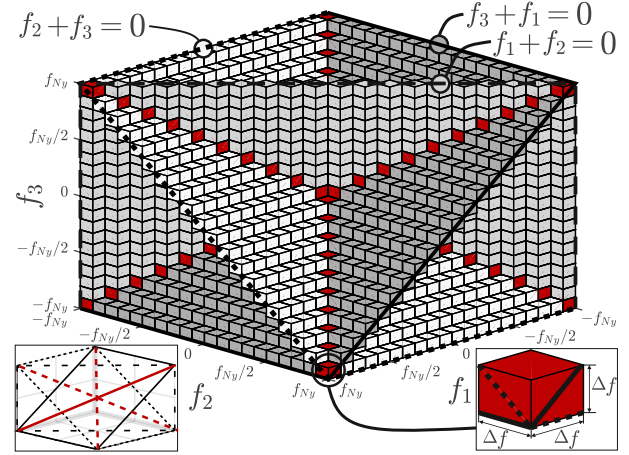


Fig. 1. SK estimates (red) and estimates (grey) containing normal manifolds (bold planes) of bandwidth Δf as subsets of the trispectral set

Defining the single-frequency fourth-order cumulant $c_4(f)$ involves the cumulant trispectrum $C_4(f, f, -f)$, which requires segregating the normal manifolds of the set (9) from the trispectrum. These manifolds refer to the second-order spectrum $S_2(f) = C_2(f)$ [13]. Integrating the spectral density of each manifold results in μ_2^2 . Since two normal manifolds intersect at the single-frequency subset (8) of the trispectrum, they are accordingly eliminated by subtracting $\mu_2^2(f)$ twice

$$c_4(f) \hat{=} (\Delta f)^3 \Re[C_4(f, f, -f)] = \mu_4(f) - 2\mu_2^2(f) \quad (12)$$

Consequently, the spectral kurtosis $SK(f)$ is defined by

$$SK(f) = \frac{c_4(f)}{c_2^2(f)} = \frac{\mu_4(f)}{\mu_2^2(f)} - 2 \quad (13)$$

A. Estimating the spectral kurtosis (SK)

Modeling transients and varying components in the frequency domain obligates an extension of the classic Fourier representation, which is fundamentally bound to stationarity. The most intuitive extensions are the evolutionary spectrum (ES) proposed by Priestley [14] and the Wold-Cramer decomposition (WCD) by Antoni [4]. The former extends the complex exponentials of the Fourier integral to amplitude-modulated complex exponentials. The latter couples a time-variant filter to a stationary white noise process. To process the

resulting data in the frequency domain requires adjustments to the Fourier analysis procedure. One form is the STFT analysis loosening the hypothesis of stationarity from the full data set to the unique segments s' . Consequently, the spectral decomposition can be observed in time.

For estimating the SK, the STFT-based estimator processes second- and fourth-order averages $(|\tilde{X}_w[k']|^n = \frac{1}{S'} \sum_{s'} |\tilde{X}_w[k', s']|^n = \frac{1}{S'} \sum_{s'} (\tilde{X}_w[k', s'] \tilde{X}_w[-k', s'])^{\frac{n}{2}}$; for even n) of the windowed STFT $\tilde{X}_w[k', s']$ for frequencies¹ k' [4]

$$\widehat{\text{SK}}_{STFT}[k'] \triangleq \frac{|\tilde{X}_w[k']|^4}{(|\tilde{X}_w[k']|^2)^2} - 2 \quad (14)$$

The estimating scheme is analogous to the STFT-estimator for HOS [6], [15]. It introduces a set of parameters relating to the segmentation, which includes the segment length S_w (defining the estimates resolution $\Delta f_{k'} = 2f_{Ny}/S_w$), the segment overlap, and the corresponding windowing function to reduce spectral leakage. Since foremost the segment length can have a substantial impact on the SK results the estimator is commonly applied for a set of different configurations visualized as the kurtogram [16].

III. FILTERING-AVERAGING (FA) ESTIMATOR FOR THE SK

While the STFT approach is intuitive in its nature to detect non-stationary components, there are further options particularly considering that HOS analysis allows to identify a varying spectral decomposition under the hypothesis of the introduced models (e.g. ES, WCD). This leads to an alternative approach for estimating the SK provided by filtering averaging (FA) [17], [7].

Following the ES, non-stationary data is the result of a stationary Gaussian process $X_g(t)$ modulated by a frequency-selective function in time $a(f, t)$. This defines $a(f, t)$ as a frequency-variant envelope operating on the underlying stationary Gaussian data $x_g(t)$. Imposed as a multiplication in the time domain, the frequency-domain equivalent is the circular convolution $X(f) = X_g(f) * A(f, f')$ of the latter's Fourier transform $X_g(f)$ with the Fourier transform $A(f, f')$ of the modulating envelope ($t \circ \bullet f'$). If $x_g(t)$ is subjected to a varying envelope (i.e. $A(f, f') \neq 0$ for $f > 0$) this introduces a phase structure into the former statistically independent phases, i.e. generates cross-frequency correlation. Applying HOS analysis to assess such a phase structure indicates that the resulting process $X(f)$ lost its conformance with the CLT.

What qualifies the SK subset for assessing such cross-frequency correlation is when $A(f, f')$ has a low-frequency evolution in f' , i.e. $a(f, t)$ varies slowly in time t . If so, the modulation (circular convolution) generates cross-frequency correlation between $X(f)$ and $X(f \pm f')$ that are decisively

¹Contrasting the fully-resolved sampling in time s and frequency k , the apostrophe indicates smoothed sampling s', k' , i.e. $\frac{1}{f_s} = \Delta t_s < \Delta t_{s'}$, $\frac{1}{T} = \Delta f_k < \Delta f_{k'}$ (sampling frequency f_s , samples S , signal duration $T = S\Delta t_s$). Further, k stands implicitly for discrete frequencies and its bandwidth Δf_k , with the latter being dropped in the notations.

localized² in the spectral domain. These cross-frequency contributions to the fourth-order moment resp. cumulant (Eq. 6) are captured by the SK subset, if the contrasting frequency bandwidth Δf of the estimates is $\Delta f > 2f'$. In practice this largely proves to be valid, since smoothing, i.e. a significant large Δf , is a fundamental principle of spectral estimation, as a premise for making the estimation of the multi-dimensional HOS computational feasible and the resulting spectral densities meaningful.

The prior passage provides the SK with a clear meaning. Under the assumption of an underlying stationary Gaussian process, SK estimates about a center frequency f capture all contributions to the fourth-order cumulant that result from a varying envelope composed of frequencies up to $f' < \Delta f/2$. Note that the divisor 'two' can be interpreted as the analogue to how the STFT estimator requires a segmentation according to the Shannon sampling theorem to capture quasi-stationary frequency components. Estimating the SK via filtering-averaging is consequently defined by (also comp. note¹)

$$\widehat{\text{SK}}_{FA}[k'] = \frac{\hat{\mu}_4[k']}{(\hat{\mu}_2[k'])^2} - 2 = \frac{(\Delta f_{k'})^3 \Re[\hat{S}_4[k', k', -k']]}{(\Delta f_{k'} \hat{S}_2[k'])^2} - 2 \quad (15)$$

Hereby, the HOS estimates are given by,

$$\hat{\mu}_4[k'] = \Re \left[\underbrace{\frac{1}{S} \sum_s x[s] x[s, k'] x[s, k'] x^*[s, k']}_{=\hat{\mu}_2[k'] = \Delta f_{k'} \hat{S}_2[k']} \right] \quad (16)$$

whereby $x[s, k'] = \sum_k H_{k'}[k - k'] X[k] e^{i2\pi ks}$ are analytic signals, which are extracted by the one-sided band-limited filter function $H_{k'}[k - k']$ for k' [7] (e.g. ideal bandpass $H_{k'}[k - k'] = 1 \forall k \in k'$, else 0).

A. Envelope analysis on SK estimates

In contrast to the STFT estimator (Eq. 14) filtering-averaging provides the SK estimates with its full time-resolution (complex-valued)

$$\hat{\mu}_4[k', s] = (\Delta f_{k'})^3 \hat{S}_4[k', k', -k', s] = x[s] x[s, k'] x[s, k'] x^*[s, k'] \quad (17)$$

Depending on the nature of the data under investigation this time-resolution may be investigated to observe the precise location of the corresponding transients in the time-domain. Likewise, the full time resolution may also be processed by envelope analysis to identify whether an SK estimate is subjected to a cyclic modulation. In other words — whether its corresponding envelope $a(f, t)$ tends to be random or deterministic (cyclo-stationary). If $a(f, t)$ provides a cyclic envelope, the envelope analysis reveals its characteristic frequencies, e.g. the damage signature of a defect rolling element bearing.

²Exemplary, cross-correlation between $X(f)X(-f + f')X(f + \varepsilon)X(-f - f' - \varepsilon)$ would be captured by the fourth-order trispectrum ($\sum_{f_1, \dots, f_4} = 0$; ε representing an infinitesimal frequency).

As a final note — carrying out band-limited analysis produces time-domain leakage. Hereby, the filter function $H_{k'}[k - k']$ defines the leakage that affects the time resolution due to frequency-domain segmentation [18].

IV. APPLICATION OF THE INTEGRATED SK ANALYSIS

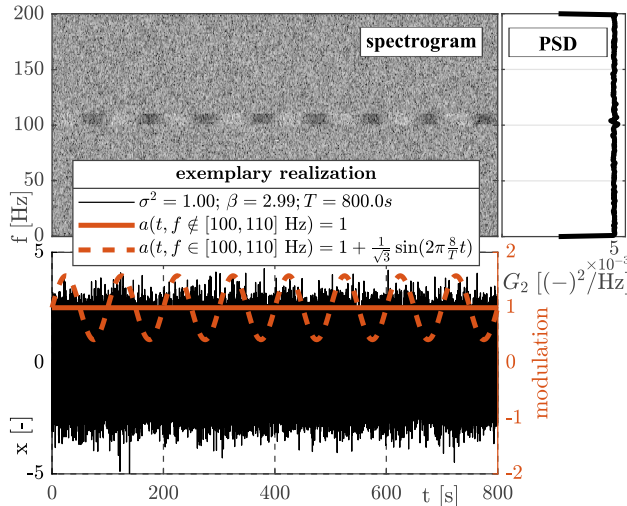


Fig. 2. Exemplary realization — broadband noise with a frequency-selective, amplitude-modulated interval $f = [100 \ 110]$ Hz

This section introduces a simple example to illustrate the FA estimation scheme and envelope analysis, but also to provide a brief comparison to the STFT estimation procedure. Therefore, Fig. 2 shows a realization of unit-variance, evenly-distributed noise. While the example is constructed to represent stationary Gaussian noise for most of its spectral decomposition, the frequency interval $f = [100, 110]$ Hz is subjected to a sine-modulation varying about one (Fig. 2). The sine’s amplitude $1/\sqrt{3}$ is chosen so that the expected value (calculated via $\overline{a(f, t)^4}/\overline{a(f, t)^2}$) is $SK(f) = 1$ for the non-stationary band ($f = [100, 110]$ Hz), while being nil $SK(f) = 0$ for the remaining stationary components. Fig. 2 further includes the time-frequency visualization (spectrogram) and the average PSD. A numerical study based on 500 realizations that were generated accordingly was carried out to compare the STFT and FA estimation techniques for a set of different configurations (Tab. I). For each configuration the mean and the standard deviation of the individual estimates were calculated to investigate the error.

Exemplary, Fig. 3 shows a comparison of the SK estimated via STFT- (Hanning window of length $S_w = 128$ and overlap of 75%) and the FA scheme (ideal band-pass of bandwidth $\Delta f_{k'} = \frac{f_s}{S_w}$ Hz resp. $\frac{2f_s}{S_w}$ Hz). The properties of STFT estimates significantly rely on tapered windows and a significant overlap. Implying such a configuration, the STFT estimator is less subjected to error noise but shows a larger bias than the FA estimator, considering the same bandwidth $\Delta f_{k'}$. Doubling the bandwidth of FA estimates reduces the error variance to a similar level but retains a smaller bias (Fig. 3).

Tab. I further includes a configuration of the FA estimator that applies a Hanning window in the frequency-domain. Incorporating a windowing function (frequency-domain) to the FA scheme trades variance against less bias. Further, establishing an overlapping scheme into the frequency discretization does not change the variance (only affected by bandwidth) but may change the bias properties, due to a more adequate center frequency. However, STFT and FA belong to the same family of periodogram estimators [7]. It can therefore be concluded, that in practice they rather differentiate by their handling than by their estimator properties. Hereby, FA

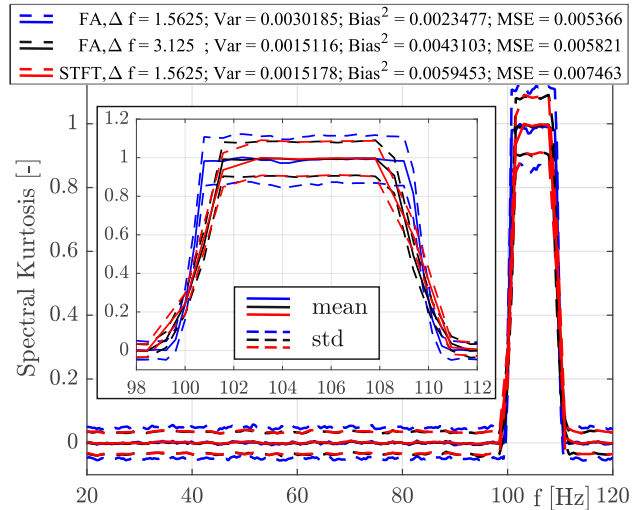


Fig. 3. Spectral Kurtosis via STFT and FA estimator

TABLE I
NUMERICAL STUDY FOR ESTIMATOR PROPERTIES

		S_w [-]	256	128	64
		$\Delta f_{k'}$ [Hz]	1.5625	3.125	6.25
FA	Var		3.02e-03	1.51e-03	7.41e-04
	Bias ²		2.35e-03	4.31e-03	1.01e-02
	MSE		5.37e-03	5.82e-03	1.08e-02
FA	Var		4.82e-03	2.42e-03	1.20e-03
	Bias ²		1.47e-03	2.72e-03	6.82e-03
	MSE		6.29e-03	5.14e-03	8.02e-03
STFT	Var		3.79e-03	1.81e-03	8.33e-04
	Bias ²		5.66e-03	1.52e-02	2.30e-02
	MSE		9.46e-03	1.70e-02	2.38e-02
STFT	Var		1.76e-03	8.42e-04	3.87e-04
	Bias ²		5.71e-03	1.52e-02	2.29e-02
	MSE		7.48e-03	1.61e-02	2.33e-02
STFT	Var		3.83e-03	1.85e-03	8.34e-04
	Bias ²		5.92e-03	1.49e-02	2.24e-02
	MSE		9.75e-03	1.67e-02	2.33e-02
STFT	Var		1.52e-03	7.07e-04	3.19e-04
	Bias ²		5.95e-03	1.50e-02	2.26e-02
	MSE		7.46e-03	1.57e-02	2.29e-02

uniquely provides an SK estimate with its full time-resolution. Exemplary, Fig. 4 illustrates the full time-resolution (equal sampling as realization) of two SK estimates by comparing a modulated (red) and a non-modulated (black) band. It further includes their cumulated sum of the fourth-order cumulants

$(c_4[k', S'] = 1/S \sum_s^{S'} c_4[k', s]$; Eq. 12) on the second y-axis. This shows how the envelope of the modulated band accumulates fourth-order moment in time (red) and how the stationary band varies about zero. Lastly, Fig. 4 shows the periodogram of the modulated band's envelope ($|\mu_4[k', s]|$, red). In contrast, the black periodogram shows the spectrum of the squared envelope, which is the result of defining the envelope directly on the fourth-order $|\mu_4[k', s]|$ without normalization (square root).

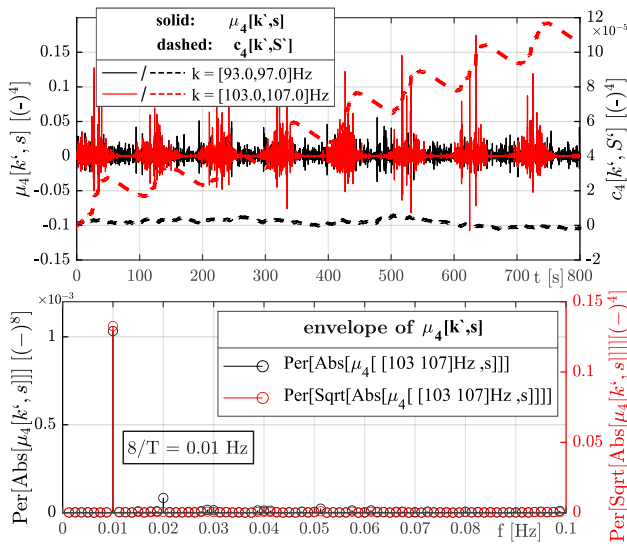


Fig. 4. Time-domain resolution and envelope analysis of SK estimates

V. CONCLUSION

In this paper the spectral kurtosis (SK) is introduced from the perspective of higher-order spectral (HOS) analysis. This complements the SK with additional insight regarding its normalization and its real-valued nature. Foremost, the tie to HOS makes existing research on HOS estimation accessible. Hereby, a new estimating scheme for the SK utilizing filtering-averaging is introduced. It bypasses the segmentation, which the popular STFT scheme is based upon, and provides the full time-resolution of SK estimates. This offers the potential to improve the bias properties, foremost for transient events that are significantly shorter than the STFT segment length. Stable estimates are obtained on the basis of a single parameter — the frequency bandwidth about a frequency of interest, which can directly be related to the spectral composition of its time envelope. The time resolution of SK estimates can further be processed to localize random transients in the estimate's time evolution or by analyzing the spectral decomposition of the envelope to identify whether the SK's value originates from a periodic modulation (cyclostationary). This integrated SK analysis may further be extended to the proposal of [19], in which the kurtosis is decomposed into a two-dimensional frequency-domain decomposition. In this form it can assess whether frequency bands, i.e. SK estimates, are subjected to a

synchronous modulation and it can directly be related to full fourth-order central moment of the underlying process.

REFERENCES

- [1] R. B. Randall and J. Antoni, "Rolling element bearing diagnostics—A tutorial," *Mechanical Systems and Signal Processing*, vol. 25, no. 2, pp. 485–520, 2011.
- [2] Y. Wang, J. Xiang, R. Markert, and M. Liang, "Spectral kurtosis for fault detection, diagnosis and prognostics of rotating machines: A review with applications," *Mechanical Systems and Signal Processing*, vol. 66-67, pp. 679–698, 2016.
- [3] R. F. Dwyer, "Detection of non-Gaussian signals by frequency domain kurtosis estimation," *IEEE International Conference on Acoustics, Speech, and Signal Processing*, pp. 607–610, 1983.
- [4] J. Antoni, "The spectral kurtosis: a useful tool for characterising non-stationary signals," *Mechanical Systems and Signal Processing*, vol. 20, no. 2, pp. 282–307, 2006.
- [5] V. Vrabie, P. Granjon, and C. Serviere, "Spectral kurtosis: from definition to application," *6th IEEE International Workshop on Nonlinear Signal and Image Processing*, 2003.
- [6] C. L. Nikias and A. P. Petropulu, *Higher-order spectra analysis: A nonlinear signal processing framework*, Prentice Hall, Englewood Cliffs, NJ, 1993.
- [7] A. Trapp and P. Wolfsteiner, "Estimating higher-order spectra via filtering-averaging," *Mechanical Systems and Signal Processing*, vol. 150, 2021.
- [8] M. J. Hinich, D. Marandino, and E. J. Sullivan, "Bispectrum of ship-radiated noise," *The Journal of the Acoustical Society of America*, vol. 85, no. 4, pp. 1512–1517, 1989.
- [9] J. W. Dalle Molle, *Higher-order spectral analysis and the trispectrum*, PhD Thesis, University of Texas, Austin, TX, 1992.
- [10] F. Hausdorff, *Beiträge zur Wahrscheinlichkeitsrechnung (Contributions to probability theory)*, Königl. Sächs. Gesellschaft der Wissenschaften zu Leipzig, 1901.
- [11] W. B. Collis, P. R. White, and J. K. Hammond, "Higher-order spectra: The bispectrum and trispectrum," *Mechanical Systems and Signal Processing*, vol. 12, no. 3, pp. 375–394, 1998.
- [12] G. Schuëller and C. Bucher, "Non-Gaussian response of systems under dynamic excitation," in *Stochastic Structural Dynamics*, S. T. Ariaratnam, Ed., pp. 219–239. Elsevier, London, 1988.
- [13] B. Picinbono, "Geometrical concepts in HOS," *Proceedings of the IEEE Signal Processing Workshop on Higher-Order Statistics*, pp. 320–327, 1999.
- [14] M. B. Priestley, "Evolutionary spectra and non-stationary processes," *Journal of the Royal Statistical Society*, vol. 27, no. 2, pp. 204–237, 1965.
- [15] J. W. Dalle Molle and M. J. Hinich, "Trispectral analysis of stationary random time series," *The Journal of the Acoustical Society of America*, vol. 97, no. 5, pp. 2963–2978, 1995.
- [16] J. Antoni and R. B. Randall, "The spectral kurtosis: application to the vibratory surveillance and diagnostics of rotating machines," *Mechanical Systems and Signal Processing*, vol. 20, no. 2, pp. 308–331, 2006.
- [17] J. Bendat and A. Piersol, *Random data: Analysis and measurement procedures*, Wiley, Hoboken, NJ, 2010.
- [18] C. C. Smith, J. F. Dahl, and R. J. Thornhill, "The duality of leakage and aliasing and improved digital spectral analysis techniques," *Journal of Dynamic Systems, Measurement, and Control*, vol. 118, no. 4, pp. 741–747, 1996.
- [19] A. Trapp and P. Wolfsteiner, "Frequency-domain characterization of varying random vibration loading by a non-stationarity matrix," *International Journal of Fatigue*, vol. 146, 2021.